Numerical study of solar-wind tower systems for ventilation of dwellings

H.F. Nouanégué, L.R. Alandji, E. Bilgen*

Ecole Polytechnique, C.P. 6079 centre ville Montreal, QC, Canada H3A 3A7

Abstract

Numerical study is carried out of a simplified system of solar-wind tower for ventilation of dwellings. The conservation equations for mass, momentum and energy for mixed convection in two-dimensional coordinates are solved by the control volume method and Simpler algorithm. The governing parameters of the problem are Rayleigh number Ra, Reynolds number, Re (or Richardson number, Ri), the dimensionless conductivity of the solid medium, k_r and the geometrical parameters. Nusselt number Nu and dimensionless volume flow rate $\dot{V}$ are calculated as a function of the governing parameters, and streamlines and isotherms are produced. The results show that the important parameters affecting the ventilation performance are Ra, Re (or Ri), and the geometrical parameters, the aspect ratio A, the exit port size h_1/L and to a lesser degree, the wall thickness ℓ_1/L.

1. Introduction

In hot and arid regions, use of conventional wind towers to achieve comfort is a well-known traditional technique. The wind towers maintain natural ventilation through living spaces due to wind as well as buoyancy effects (see, e.g., [1]). The mechanisms of functioning and operation of wind towers depends on (i) the time of operation, nights or day time, (ii) the availability of wind, i.e. windy or not windy periods, (iii) the type of wind towers. In addition, they are only used in summer time and closed down in winter. Description and operation of various cases are described; advantages and operational problems are discussed [1]. An experimental study with actual wind towers is reported by Yaghoubi et al. [2]. They found that the wind towers were effective not only in strong wind but also in calm weather by providing a certain air circulation to provide comfort in dwellings. At downside, they found that when the tower was subject to strong solar radiation and the tower structure was heated up, the circulating air was heated up by hot surfaces causing discomfort. Experimental studies [3,4] and a numerical study [5] on

the solar chimney for ventilation were also reported. The results of these studies showed that ventilation by solar chimney was possible; the mass flow rate was increasing function of chimney surface temperature, reverse flow was observed for certain channel sizes and the ventilation increased with increasing inlet port size. In another study, Bansal et al. [6] proposed to use an open-ended solar collector system installed separately from the wind tower. Their results show that the effect of solar system is more important than that of wind and the combined system may be more effective in ventilating living quarters by increasing the mass flow rate of air by several times.

The conventional wind tower can be conceived as a combination of solar and wind tower for ventilation of dwellings. In this case, the tower does not function as a wind catcher but it rather functions as a chimney for ventilating air from the dwelling. The opening at the top is oriented against the cardinal wind direction, thus it will be in depression region most of the time. The tower itself can be used as a solar collector and energy storage system, at the same time providing wind tower function (see Fig. 1(a)). The air will be evacuated from the dwelling to the ambient by suction in the tower due to negative wind pressure at the opening (the so-called venturi effect) and due to the buoyancy force developed in the chimney by hot

---

*Corresponding author. Tel.: +514 340 4711x4579 fax: +514 340 5917.
E-mail address: bilgen@polymtl.ca (E. Bilgen).

Nomenclature

A	aspect ratio, H/L
c_p	heat capacity, J/kg K
g	acceleration due to gravity, m/s
H	tower height, m
h_1, h_2	exit and entrance port size
k	thermal conductivity, W/mK
k_r	solid to fluid thermal conductivity ratio, $= k/k_f$
L	tower width, m
ℓ_1	wall thickness, m
Nu	Nusselt number, $= hL/k$
p	pressure, Pa
P	dimensionless pressure, $= p/\rho U_o^2$
Pr	Prandtl number, $= \upsilon/\alpha$
q''	heat flux, W/m^2
q	dimensionless heat flux, $= \partial\theta/\partial X$
Ra	Rayleigh number, $= g\beta q'' L^4/(\upsilon\alpha k)$
Re	Reynolds number, $= U_o L/\upsilon$
T	temperature, K
ΔT	temperature difference, $= q'' L^2/\rho C_p U_o$
t	time, s
U, V	dimensionless fluid velocities, $= u/U_o, v/U_o$
U_o	forced convection velocity, m/s
$\dot{V}$	dimensionless volume flow rate through the openings

X, Y	dimensionless Cartesian coordinates, $= x/L$, y/L,
x, y	Cartesian coordinates

Greek symbols

α	thermal diffusivity, m^2/s
β	volumetric coefficient of thermal expansion, 1/K
υ	kinematic viscosity, m^2/s
ρ	fluid density, kg/m^3
Ψ	dimensionless stream function
θ	dimensionless temperature, $= (T - T_\infty)/\Delta T$
τ	dimensionless time, $t/(L/U_o)$

Superscripts

—	average

Subscripts

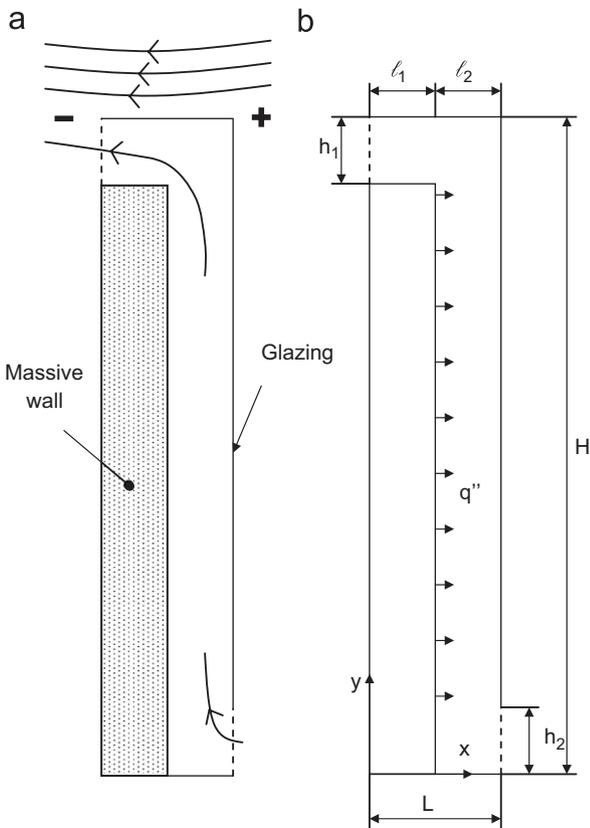|	
a	air
f	fluid
max	maximum
min	minimum
∞	ambient value

Fig. 1. Schematic of the simplified solar-wind tower computational domain and coordinate system.

surfaces, usually a combination of both. Similar to classical wind tower applications, a typical solar-wind tower may be 10–20 m high and 1–3 m on each side for a rectangular cross section or equivalent average diameter for a quasi-circular cross section.

In this article, we will carry out a numerical study on a simplified solar-wind tower of the type described above and determine governing parameters affecting its performance.

2. Problem definition and mathematical model

A two-dimensional schematic of the simplified solar-wind tower geometry and coordinate system is shown in Fig. 1(b). The two horizontal and the left solid boundaries of the tower in Fig. 1(b) are adiabatic and the right boundary adjacent to the vertical air channel is isothermal. The latter represents glazing for reception of solar radiation and the massive wall on the left is a structural component, which is used as energy storage (Fig. 1(a)). As explained in the Introduction, the wind current will create a negative pressure at the tower outlet by the so-called venturi effect, which will result in a forced convection in the tower system. The solar energy absorbed by the massive wall and its subsequent release will create a natural convection. Thus, the flow in the tower system will be combination of these two modes, i.e. by mixed convection. The boundary conditions including those at the two

openings will be presented at the end of the mathematical model.

In this study, the aspect ratio, $A = H/L$, the massive wall thickness, ℓ_1/L, the exit port height, h_1/L and the non-dimensional massive wall conductivity, $k_r = k/k_f$ will be taken as variable. The air channel width, $\ell_2/L = 0.5$ and the inlet port size, $h_2/L = 1.05$ will be kept constant. Due to combined effects of wind and solar

energy, and inclusion of the massive wall, we will have a conjugate heat transfer by mixed convection and conduction in the tower.

We note that our aim in this study is to establish the effect of governing parameters on the system thermal performance and to do it we use a simplified system with the following assumptions: the effect of the third dimension is negligible like in the solar collector systems with a massive wall, the flow mode is laminar, which is most of the time justified for systems with small channel size and small velocities (see, e.g. [7]), and infrared radiation heat exchange in the channel is negligible. With these assumptions, two-dimensional conservation equations for mass, momentum and energy are used with Boussinesq approximation. By choosing L as the length scale, U_o as the velocity scale, $\Delta T = q''L^2/\rho C_p U_o$ as the temperature scale, ρU_o^2 as the pressure scale and $t/(L/U_o)$ as the time scale, we obtain following dimensionless equations in terms of dimensionless primitive variables for mixed convection

Table 1
Comparison of the results for free convection between vertical plates

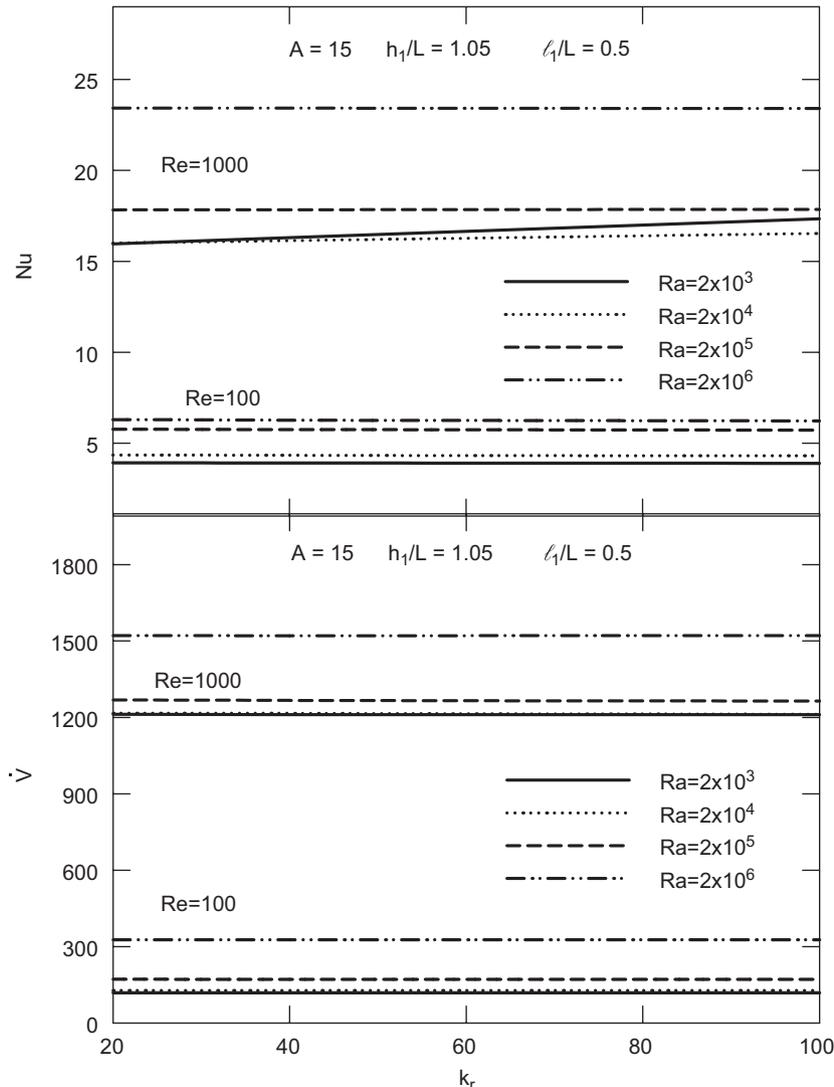| Ra/A	$Nu/2A$ [10]	$Nu/2A$ (this study)
10^0	0.0403	0.04100
10^1	0.3780	0.3700
10^2	1.8518	1.8420
10^3	4.1660	4.1790
10^4	7.4686	7.5200

Fig. 2. Nusselt number and volume flow rate $\dot{V}$ as a function of wall conductivity k_r for the base case of $A = 15$, $h_1/L = 1.05$, $\ell_1/L = 0.5$, and Rayleigh and Reynolds numbers as variable parameters.

and conduction

$$\frac{\partial U}{\partial X} + \frac{\partial V}{\partial Y} = 0, \tag{1}$$

$$\frac{\partial U}{\partial \tau} + \frac{U \partial U}{\partial X} + \frac{V \partial U}{\partial Y} = -\frac{\partial P}{\partial X} + \frac{1}{Re}\left(\frac{\partial^2 U}{\partial X^2} + \frac{\partial^2 U}{\partial Y^2}\right), \tag{2}$$

$$\frac{\partial V}{\partial \tau} + \frac{U \partial V}{\partial X} + \frac{V \partial V}{\partial Y} = -\frac{\partial P}{\partial Y} + \frac{1}{Re}\left(\frac{\partial^2 V}{\partial X^2} + \frac{\partial^2 V}{\partial Y^2}\right) + \frac{Ra}{Pr\, Re^2}\,\theta, \tag{3}$$

$$\frac{\partial \theta}{\partial \tau} + \frac{U \partial \theta}{\partial X} + \frac{V \partial \theta}{\partial Y} = \frac{\lambda}{Pr\, Re}\left(\frac{\partial^2 \theta}{\partial X^2} + \frac{\partial^2 \theta}{\partial Y^2}\right) + 1, \tag{4}$$

where λ is equal to k_r for solid media and 1 for fluid media.

The governing parameters of the problem are Ra, Re (or $Ri = Ra/Re^2$ as seen in Eqs. (2)–(3)) and Pr, which are defined in the Nomenclature. In addition, $A = H/L$, ℓ_1/L,

h_1/L are the geometric parameters and k_r is the thermal parameter.

The average Nusselt number at the exit port is calculated as

$$\overline{Nu} = \frac{-\int_{1-h_1/L}^{1}(-(\partial\theta/\partial X) + Pr\, Re\, U\theta)\,\mathrm{d}Y}{\int_{1-h_1/L}^{1}\theta\,\mathrm{d}Y}. \tag{5}$$

The volume flow rate, $\dot{V}$ is calculated as

$$\dot{V} = -\int_{x=0} U\,\mathrm{d}Y. \tag{6}$$

The stream function is calculated from its definition as

$$U = -\frac{\partial \psi}{\partial Y}, \quad V = \frac{\partial \psi}{\partial X}. \tag{7}$$

ψ is zero on the solid surfaces and the streamlines are drawn by $\Delta\psi = (\psi_{max} - \psi_{min})/n$ where n is the number of increments.
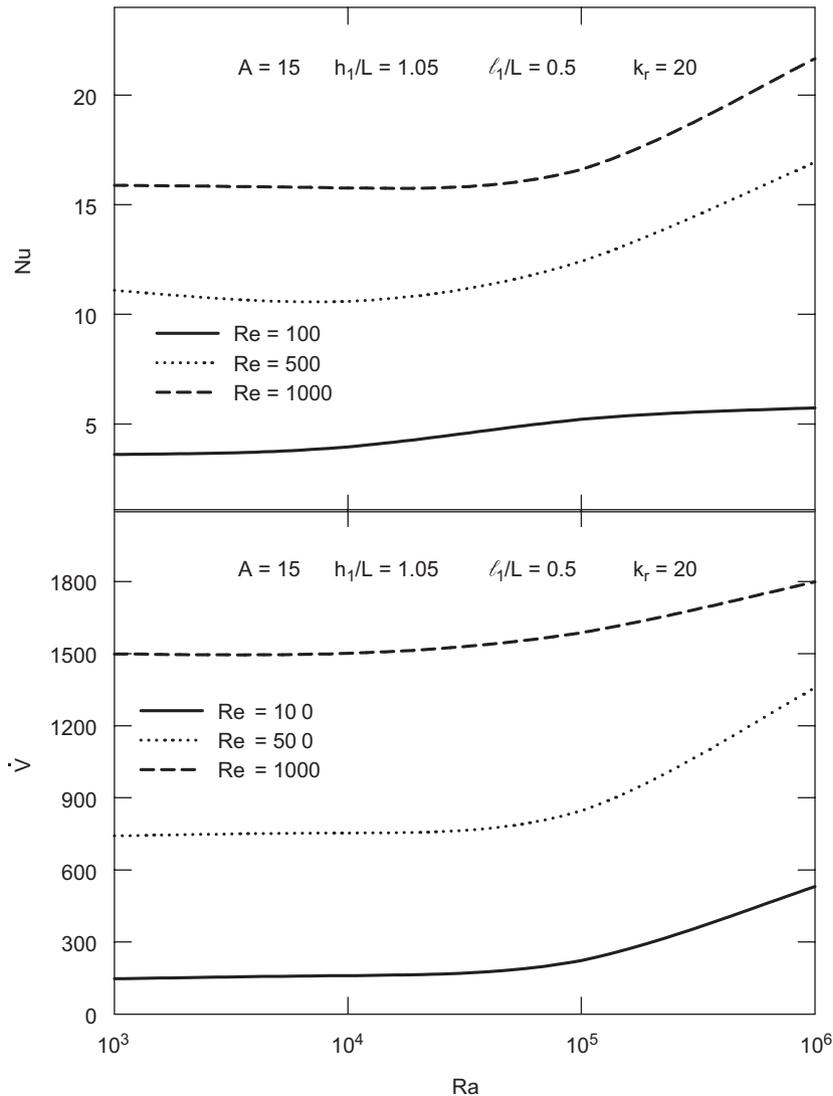

Fig. 3. Nusselt number and volume flow rate $\dot{V}$ as a function of Rayleigh number for the case of $A = 15$, $h_1/L = 1.05$, $\ell_1/L = 0.5$, $k_r = 20$ and Reynolds number as variable parameter.

Boundary conditions in terms of dimensionless variables are

On all solid surfaces : $\quad U = 0, \quad V = 0,$ (8)

On adiabatic walls : $\quad \dfrac{\partial \theta}{\partial Y} = 0,$ (9)

At the inlet port : $\quad U = -1, \quad \theta = 0,$ (10)

At the exit port : $\quad \dfrac{\partial V}{\partial X} = 0, \quad \dfrac{\partial U}{\partial X} = -\dfrac{\partial V}{\partial Y},$

$\left(\dfrac{\partial \theta}{\partial X} \right) = 0.$ (11)

The dimensionless heat flux on the solid wall is

$q = \dfrac{\partial \theta}{\partial X} = 1.$ (12)

3. Numerical method

The numerical method used to solve Eqs. (1)–(4) with the boundary conditions Eqs. (8)–(11) is the Simpler (semi-implicit method for pressure linked equations revised) algorithm [8]. The computer code based on the mathematical formulation presented above and the Simpler method were validated earlier with respect to the benchmark [9]. The results showed that the general concordance was excellent. For example, the deviations in Nusselt number and the maximum stream function at $Ra = 10^6$ were 0.60% and 1.39%, respectively. A validation study was also conducted with respect to the results of a differentially heated vertical open channel [10]. The result of this validation is presented in Table 1, where we can see that the agreement is very good.

Grid convergence was studied for the case of $A = 15$ with uniform grid sizes from 10×150 to 20×300 at $Ra = 10^5$ and $Re = 20$. Grid independence was achieved with grid size
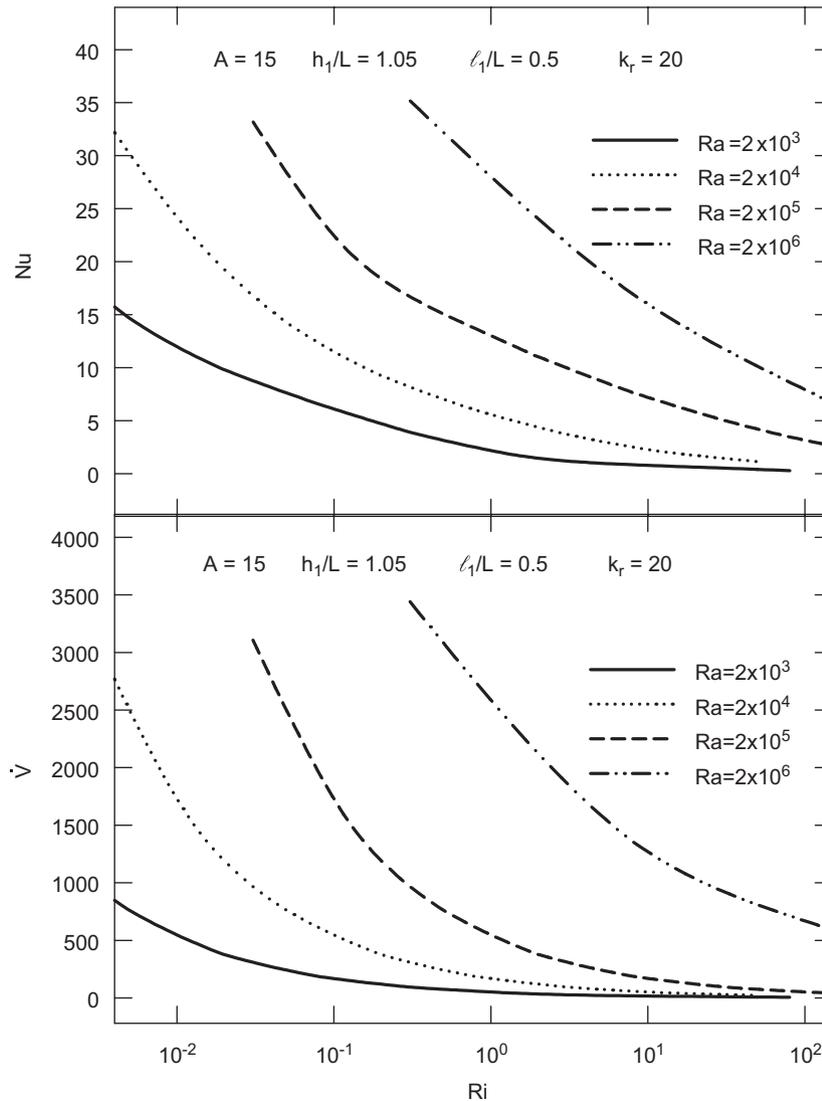

Fig. 4. Nusselt number and volume flow rate $\dot{V}$ as a function of Richardson number for the case of $A = 15$, $h_1/L = 1.05$, $\ell_1/L = 0.5$, $k_r = 20$ and Rayleigh number as variable parameter.

of 20×200 within 0.065% in Nusselt number and 0.094% in extremum stream function. Using a system with a mobile processor of 2 GHz clock speed, for $A = 15$, 20×200 grid size, at $Ra = 10^6$, the typical execution time was 218 s.

A converged steady-state solution was obtained by iterating in time until variations in the primitive variables between subsequent time steps were very small

$$\sum(\phi_{i,j}^{\text{old}} - \phi_{i,j}) < 10^{-4}, \tag{13}$$

where ϕ stands for U, V, and θ.

Within the same time step, residual of the pressure term was less than 10^{-3} [7,8]. In addition, the accuracy of the solution was double checked using the energy conservation on the domain to ensure it was less than 10^{-4}.

4. Results and discussion

Non-dimensional geometrical parameters are based on the experience with the Trombe wall systems with ventilation: typical dimensional values are $\ell_1 =$ 0.10 m massive wall thickness, $\ell_2 = 0.10$ m air channel width, $H = 2$–4 m height and fairly large entrance and exit ports to reduce the flow resistance of air to and from dwellings (see, e.g. [11]). Thus, we carried out the numerical study with the air channel width, $\ell_2/L = 0.5 = \text{constant}$ and the size of the inlet air port, $h_2/L = 1.05 = \text{constant}$. We varied the other parameters as follows: the aspect ratio, $A = H/L$ from 10 to 20, the massive wall thickness, ℓ_1/L from 0.1 to 0.6, the massive wall's non-dimensional conductivity, $k_r = k/k_f$ from 20 to 100, the exit port height, h_1/L from 0.75 to 1.5. Rayleigh number is varied from 10^3 to 10^6, Reynolds number from 10^2 to 10^3. Pr is constant at 0.71 for air. The results will be presented as the Nusselt number and the volume flow rate as a function of the other parameters, the streamlines and isotherms will be presented to visualize the flow and temperature fields. The base case is with $A = 15$, $h_1/L = 1.05$, $\ell_1/L = 0.5$. Then we will present sensitivity studies for each parameter.
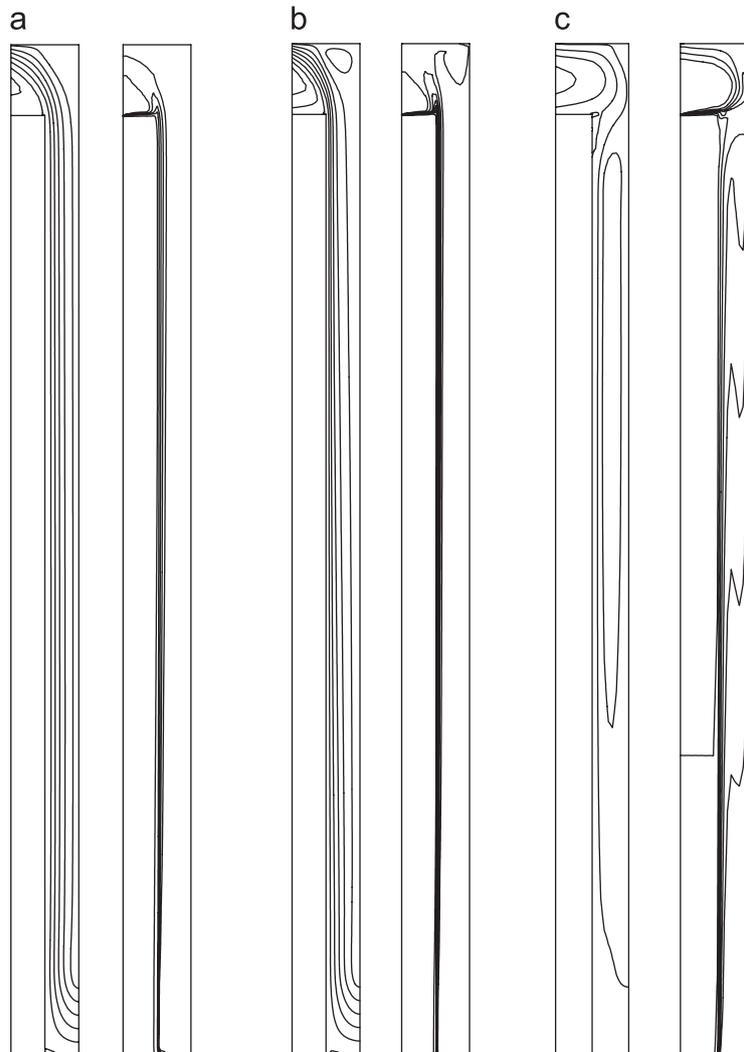

Fig. 5. Streamlines and isotherms for the case of $A = 15$, $h_1/L = 1.05$, $\ell_1/L = 0.5$, $k_r = 20$. (a) $Ri = 0.1$, (b) $Ri = 1$ and (c) $Ri = 100$. Streamlines are shown on the left and isotherms on right for each case.

We present for the base case Nusselt number, Nu and volume flow rate $\dot{V}$ through the exit port as a function of conductivity ratio, k_r with Ra and Re parameters in Fig. 2. We see that Nu and $\dot{V}$ are not too sensitive to the variation of k_r. We conclude that k_r is not an important parameter and we can take a typical value and evaluate the other parameters. The reason is that the boundary condition is adiabatic along the massive wall at $x = 0$ and k_r is only important in storing and releasing energy from the wall to the air circulating through the channel. Thus, we take $k_r = 20$ for the rest of the study and the base case becomes with $A = 15$, $h_1/L = 1.05$, $\ell_1/L = 0.5$, $k_r = 20$.

For the base case, we present Nusselt and volume flow rate as a function of Rayleigh number in Fig. 3, where Reynolds number is a parameter. We see that Nu and $\dot{V}$ are increasing with increasing Re number at all Ra numbers. As expected, for a given Re number, at low Ra numbers Nu and $\dot{V}$ are quasi-invariant to it, since we have conduction dominated natural convection regime. At higher Ra number greater than 10^5, Nu and $\dot{V}$ become an increasing function of it. The cross plot of the same data in Fig. 3, Nu and $\dot{V}$ as a function of Re number with Ra as a parameter showed that both Nu and $\dot{V}$ were increasing function of Re and Ra numbers. These observations are expected since the tower system should perform better when both Ra and Re numbers are high, the first indicating the thermal effect and the second, the forced convective flow effect on the mixed convection and ventilation.

We present Nu and $\dot{V}$ as a function of Richardson number, $Ri = Ra/Re^2$ in Fig. 4 for the base case and for four Ra numbers. We can see that both Nu and $\dot{V}$ are decreasing function of Ri for a given Ra number. As expected, for $Ri < 1$, Nu and $\dot{V}$ are strong function of Ri for a given Ra number. They decrease with increasing Ri number until about $Ri \cong 1$ thereafter, for $Ri > 1$ they converge to an asymptotic value. In addition, for higher Ra numbers, the observed dependence of Nu and $\dot{V}$ on Ri is amplified. The dependence of Nu and $\dot{V}$ on Richardson
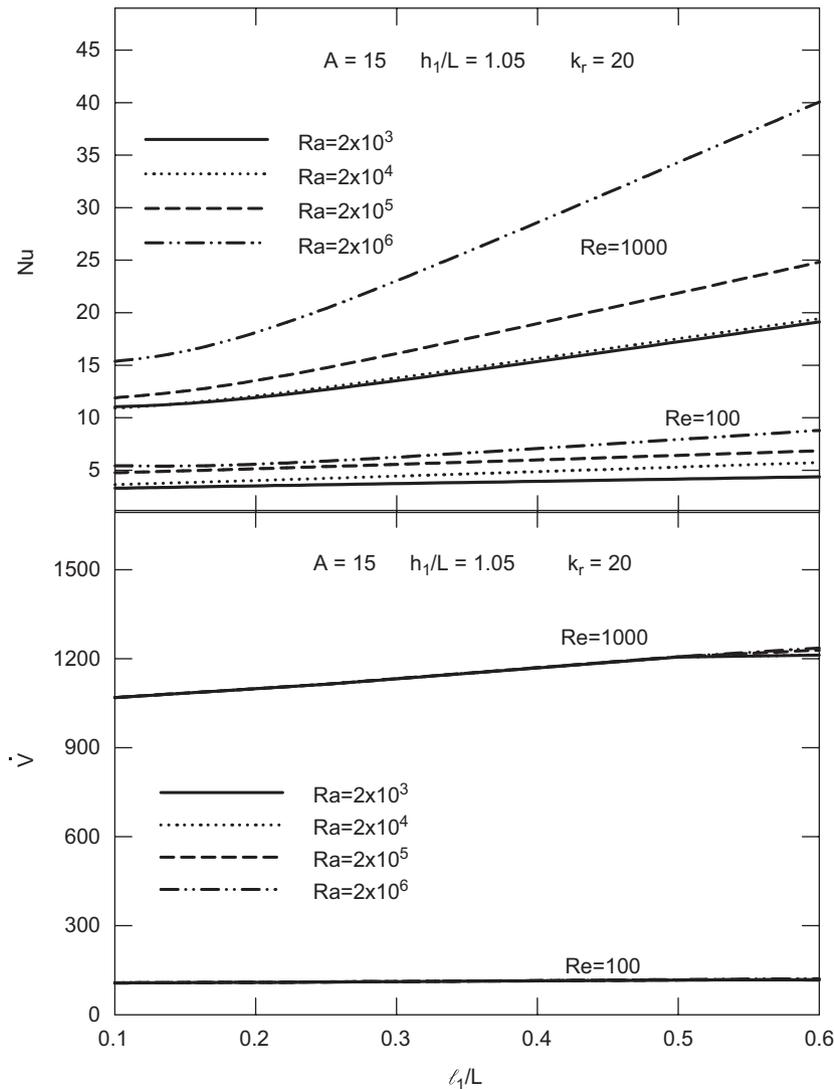

Fig. 6. Nusselt number and volume flow rate $\dot{V}$ as a function of wall thickness ℓ_1/L for the case of $A = 15$, $h_1/L = 1.05$, $k_r = 20$, and Rayleigh and Reynolds numbers as variable parameters.

number is explained by the fact that forced convection is the dominant mode for $Ri<1$, the natural convection becomes the dominant mode for $Ri>1$ and both forced and natural convections have equal importance for $Ri\cong 1$. We examine the flow and temperature fields for these three modes in Fig. 5. Again for the base case with $A = 15$, $h_1/L = 1.05$, $\ell_1/L = 0.5$, $k_r = 20$ and three cases are shown: (a) $Ri = Ra/Re^2 = 10^5/(10^3)^2 = 0.1$, (b) $Ri = 10^6/(10^3)^2 = 1$ and (c) $Ri = 10^6/(10^2)^2 = 100$. The streamlines are shown on the left and the isotherms on the right for each case. We see that for (a) $Ri = 0.1$ there is a strong convection with some reverse flow at the exit and the cooling of the heated surface is effectively with high gradients on the surface. This case is forced convection-dominated mixed convection. For (b) $Ri = 1$, both forced and natural convections play an important role with high-temperature gradient on the surface. We note that due to additional contribution by natural convection, the reverse flow at the exit is amplified.

In case (c) $Ri = 100$, both flow and temperature fields show natural convection-dominated mixed convection. There is clearly a reverse flow at the exit and the isotherms show stratification in the air channel. Compared with case (b), which is also with $Ra = 10^6$, the effect of forced convection is not discernible and we have a less favorable ventilation in the tower.

Next, we will present the results of the sensitivity study on the wall thickness ℓ_1/L, the exit port size h_1/L and the aspect ratio A.

Fig. 6 shows Nu and $\dot{V}$ as a function of the wall thickness, ℓ_1/L with Re and Ra as parameters. At small wall thickness, Nu is not too sensitive to the variation of ℓ_1/L. At high ℓ_1/L, the same trend is observed at low Re number. Nu is a strong function of ℓ_1/L at its higher values and when Re number is high. The effect of Ra number is mixed although it is a little higher at low Ra numbers at both Re numbers. The volume flow rate, $\dot{V}$ is insensitive to
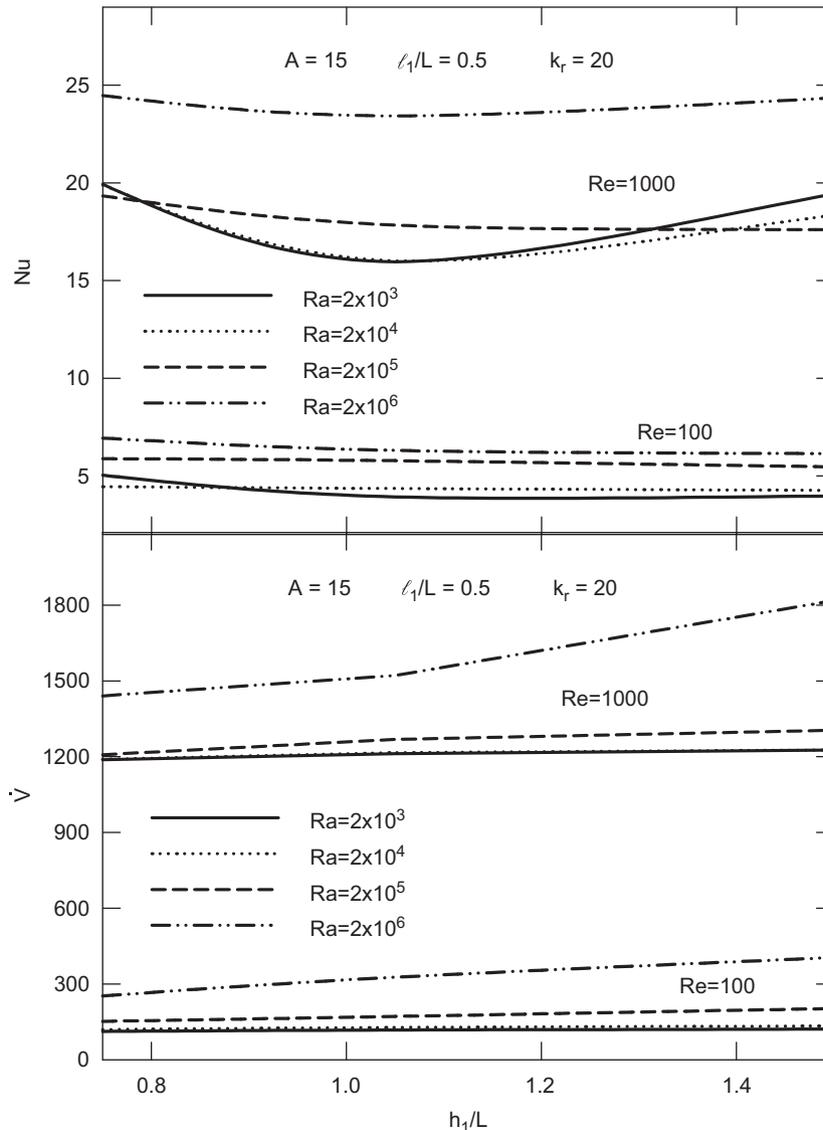

Fig. 7. Nusselt number and volume flow rate $\dot{V}$ as a function of exit port size h_1/L for the case of $A = 15$, $\ell_1/L = 0.5$, $k_r = 20$, and Rayleigh and Reynolds numbers as variable parameters.

the variation of ℓ_1/L at low Re number, and it is a gradually increasing function of it at high Re number. It is insensitive to Ra number.

We present the effect of the exit port size, h_1/L on Nu and $\dot{V}$ with Ra and Re parameters in Fig. 7. We can see that Nu and $\dot{V}$ are gradually increasing function of h_1/L for both Ra and Re numbers. Following our earlier observation in Fig. 3, the effect of h_1/L is more important at high Ra and Re numbers. This is expected because to prevent choking at the exit we need larger exit port size when the mixed convection and ventilation are increased.

The effect of the aspect ratio, A on Nu and $\dot{V}$ is shown in Fig. 8 where Ra and Re are parameters. We observe that Nu is a decreasing function of A while $\dot{V}$ is slightly increasing function of it, i.e. there is an inverse relationship. Indeed, it is a known practical observation to have an increased draft when a chimney is taller. On the other hand, for an increased draft the heat transfer at the exit is decreased for a given amount of energy transported through the chimney. We note also that depending on the operation conditions, there may be optimum aspect ratio to obtain the best ventilation performance, as seen for the case of $Ra < 10^6$ and $Re = 10^3$, for example.

5. Conclusions

We carried out a numerical study on a solar-wind tower system for ventilation of dwellings. We solved the equations for the conservation of mass, momentum and energy using the control volume method. The governing parameters are Rayleigh and Reynolds numbers (or Richardson number) and constant Prandtl for air; the geometrical parameters are the aspect ratio, the exit port size, the wall thickness and the wall conductivity. Our aim has been to establish important parameters affecting the ventilation performance of the solar-wind tower systems
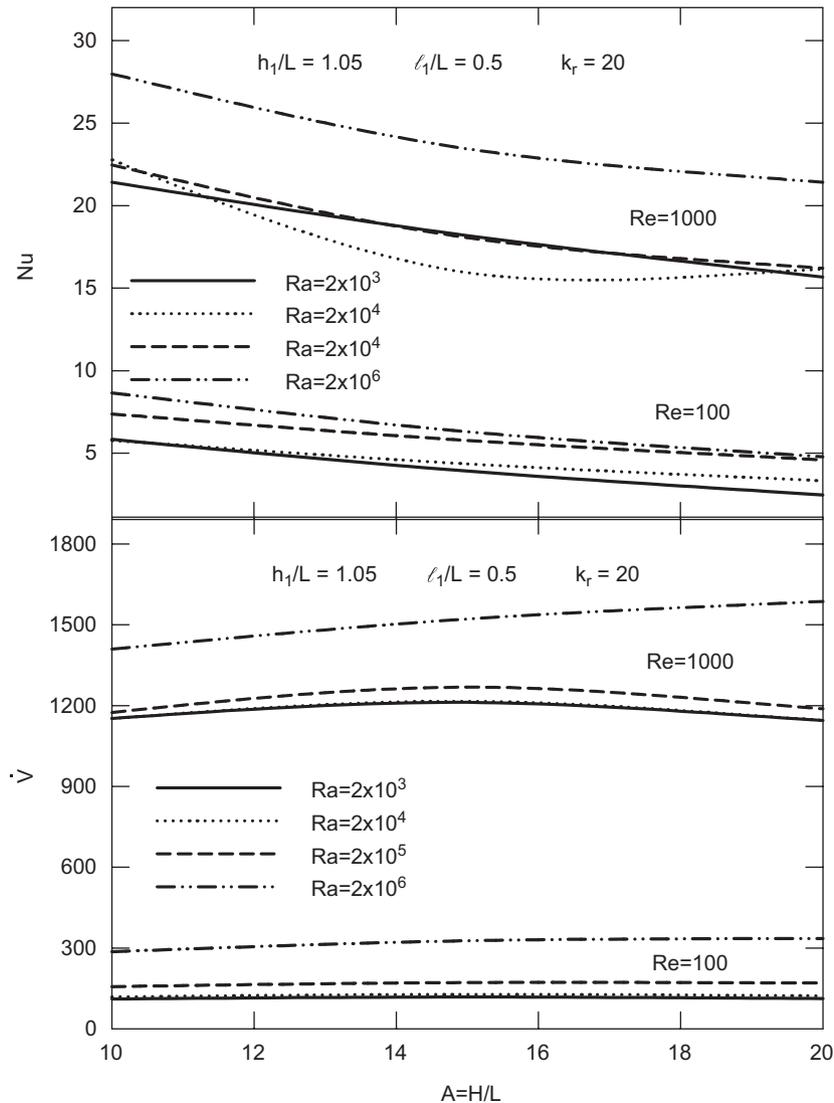

Fig. 8. Nusselt number and volume flow rate $\dot{V}$ as a function of aspect ratio A for the case of $h_1/L = 1.05$, $\ell_1/L = 0.5$, $k_r = 20$, and Rayleigh and Reynolds numbers as variable parameters.

considered in our study. In view of the results, and for the simplified system and the boundary conditions considered in this study, we summarize the following conclusions:

(i) The wall conductivity is not a major parameter. We note, however, that from the thermal storage point of view and considering that these systems will be operated in 24 h cycle, the wall conductivity should be $k_r = 20$–40, which is the range for typical construction materials.

(ii) As noted in the presented results, Richardson number is an important parameter affecting the ventilation performance. The results showed that these systems perform best for $Ri < 1$, for which the heat transfer mode is by forced convection-dominated mixed convection. It is also shown that the ventilation performance is augmented at higher Rayleigh numbers, i.e. by high natural convection contribution.

(iii) The effect of the wall thickness is negligible on the ventilation performance for low Reynolds numbers; it becomes important at high Reynolds numbers. We note that considering 24 h cyclic operation, the wall thickness should be optimized, which may correspond to $\ell_1/L = 0.5$–0.6 in this study.

(iv) The effect of the exit port on the ventilation performance is important at high Rayleigh and Reynolds numbers.

(v) The ventilation performance increases proportionately with the tower aspect ratio, particularly at high Rayleigh numbers. It is found that in this case also the aspect ratio should be optimized for the best ventilation performance.

(vi) Generally, for a given location, material used in tower construction and operation condition, the geometrical parameters, A, h_1/L and ℓ_1/L should be optimized.

References

[1] Bahadori MN. Passive cooling system in Iranian architecture. Sci Am 1978;238(2):144–52.

[2] Yaghoubi MA, Sabzevari A, Golneshan AA. Wind towers: measurement and performance. Sol Energy 1991;47(2):97–106.

[3] Bilgen E, Chaaban M. Solar heating–ventilating system using a solar chimney. Sol Energy 1982;28(3):227–33.

[4] Bouchair A. Solar chimney for promoting cooling ventilation in southern Algeria. Build Serv Eng Res Technol 1994;18(2): 81–93.

[5] Gan G, Riffat SB. A numerical study of solar chimney for natural ventilation of buildings with heat recovery. Appl Therm Eng 1998;18:1171–87.

[6] Bansal NK, Mathur R, Bhandari MS. A study of solar chimney assisted wind tower system for natural ventilation in buildings. Build Environ 1994;29(4):495–500.

[7] Detuncq B, Bilgen E. Étude expérimentale d'un capteur solaire du type Trombe et validation des relations théoriques. Trans CSME 1984;8(1):35–9.

[8] Patankar SV. Numerical heat transfer and fluid flow. Hemisphere Publishing Corporation; 1980.

[9] Bilgen E, Ben Yedder R. Natural convection in enclosure with heating and cooling by sinusoidal temperature profiles on one side. Int J Heat Mass Transfer 2006.

[10] Aung W, Fletcher LS, Sernas V. Developing laminar free convection between flat plates with asymmetric heating. Int J Heat Mass Transfer 1972;15:2293–308.

[11] Bilgen E, Michel J. Integration of solar systems in architectural and urban design. In: Sayigh AAM, editor. Sol Energy Appl Build. New York: Academic Press; 1979 [chapter 19].